Cross-Laminated Secondary Timber: Validation of Non-destructive Assessment of Structural Properties by Full-scale Bending Tests

Wenchen Dong, Colin M. Rose, Julia A. Stegemann

Department of Civil, Environmental & Geomatic Engineering, University College London, Gower Street, London, WC1E 6BT United Kingdom

Abstract

The demolition of buildings creates a vast quantity of secondary timber, which is currently chipped, downcycled or incinerated. This study examines a higher value use of secondary timber as lamellae for cross-laminated timber (CLT), which will address the increasing demand for wood products that is expected in the coming decades. The longitudinal vibration test method was used to determine the dynamic modulus of elasticity (dMoE) for secondary timber. Then, four-point bending tests were conducted for the secondary timber to obtain the static modulus of elasticity (sMoE) and modulus of rupture (MoR). The test results showed a good linear relationship between dMoE and sMoE, so the dMoE results could be used to predict sMoE of secondary timber. Furthermore, the static bending stiffness of cross-laminated secondary timber (CLST), $sMoE_{CL}$, was predicted by the dMoE from transverse vibration tests of CLST and longitudinal vibration tests of secondary timber. Four-point bending tests of CLST showed that the latter predicted $sMoE_{CL}$ more accurately. CLST panels were also found to meet the structural requirements in relevant standards. Finally, analytical models were used to predict the bending stiffness and strength of CLST. The closest prediction came from combining the shear analogy method and bearing model for CLT. This paper demonstrates the feasibility of using secondary timber as a feedstock for CLT/CLST production.

Keywords: bending strength; circular economy; mass timber; non-destructive testing; recovered timber; wood waste.

1 Introduction

Globally, the construction industry is estimated to be responsible for 40% of all material resource use and 40% of all waste generated [1]. In the United Kingdom (UK), about 67.8 million tonnes of construction and demolition (C&D) waste (30% of total UK waste) was generated in 2018 [2]. Whilst the mass of wood waste as a proportion of total C&D waste is overshadowed by mineral wastes, it is still generated in very large quantities (e.g., 4.5 Mtpa in the UK [3]). Although this resource is to some extent managed according to the cascading principle that is part of a circular economy [4,5], the recycling potential of structural members at high value is not maximised. In the UK, around 32% of timber waste undergoes open-loop downcycling to non-structural particle-based products, 56% is incinerated for energy generation, 3% is exported and 9% is incinerated without energy recovery or disposed to landfill [6,7].

Structural use of secondary timber is therefore attracting great research interest [8–10]. One challenge of reusing secondary timber for structural purposes is the potential degradation of its mechanical properties. Studies of the effects of time on the mechanical properties of timber were first systematically carried out in Japan in the 1950s [11]. However, research into the effect of timber loading history has been developing slowly. A detailed review conducted by Cavalli et al. [12] in 2016 showed that the results in the literature were not always consistent due to the uncertainty of the loading history and the unknown original mechanical properties. Nevertheless, while most research reported an unchanged modulus of elasticity (MoE), a reduced modulus of rupture (MoR) for structural timber when compared with primary timber indicated an influence of the duration of the load (DoL) on strength. For example, the examination of 991 full-size lumber tests from the United States Department of Agriculture also showed lower MoR for secondary timber than the specified value from standards for primary timber [13]. Crews and Mackenzie [14] tested 220 pieces of secondary timber with different dimensions and defects. The results showed them to have a similar MoE as new materials but a 35% and 50% reduction in MoR for low and heavy-magnitude loading, respectively. They suggested decreasing the grade assigned to secondary timber by one to two grades, relative to the values indicated by Australian visual grading standards, to reflect the MoR degradation due to DoL and defects like nail holes. This structural property degradation negatively affects the potential to directly reuse secondary timber as structural members. Moreover, secondary timber usually has aged surfaces and larger deviations of dimensions, so it cannot meet the tolerance required for cross-sections of structural members, such as those in EN 336 [15]. Secondary timber can come in shorter lengths after on-site cutting and removing parts that contain contaminants like metal fixings. Processing, such as planing and finger jointing, is often required to reach consistent cross-sectional dimensions and sufficient lengths for structural use.

Although some properties of secondary timber may be compromised when compared to primary timber, the increasing use of high-performance engineered wood products, such as cross-laminated timber (CLT), provides other opportunities for structural reuse of secondary timber [16]. The homogenisation of properties that occurs when timber elements are combined in several layers with perpendicular grain orientation in CLT reduces the influence of defects on final product properties [17,18], potentially allowing low-grade timber to be used in structures.

Relevant research has investigated the utilization of low-grade local species that are not currently considered eligible as structural materials to produce CLT, as summarised by Rose et al. [19]. Fredriksson et al. [20] presented that an increased yield of CLT could be achieved with small-diameter logs through the trapeze edging method. Lawrence [21] and Jahedi [22] showed that low-value Ponderosa pine lumber had the potential to be used in project-specific CLT grades for low-rise buildings [23]. Ma et al. [24] tested CLT made of low-value white spruce and sugar maple. The hybrid CLT provided better structural performance than standard CLT made with spruce-pine-fir. These results are promising for reuse of secondary timber with lower strength and smaller dimensions than structural timber to produce CLT, a new product that we call cross-laminated secondary timber (CLST). In addition, emerging commercial equipment [25] is boosting the processing speed for secondary timber, such as metal fixing detection and removal, which will allow sufficient quantities of secondary timber for CLST manufacture to be produced economically.

The first attempt to produce CLST on a small scale was made by Rose et al. [19]. CLST showed similar compressive strength and stiffness to a control made with primary timber, and minor defects had a small effect on the stiffness. In addition, it was suggested to replace transverse layers with secondary timber for minimising the bending stiffness reduction. Stenstad [26] used secondary timber as transverse layers to produce nine CLST specimens. The tests showed that the defects in the transverse layers for 3-ply CLT did not affect the overall bending stiffness. Arbelaez [27] also used secondary timber in the transverse layers only, and also in all layers, of full-size CLST panels. Three replicates were conducted for each layup and the results showed that they could meet all E3 grade 3-ply CLT benchmarks as per American CLT standard PRG 320 [28] although they experienced a problem with delamination failure. Ma et al. [29] tested 17 CST panels made from salvaged beetle-killed white spruce. The tests showed that the deterioration caused by budworm activities reduced bending strength and shear modulus, but the CLT panels provided adequate flexural performance as per PRG 320 [28].

Llana et al. [30] manufactured 12 CLST panels made from salvaged European oak. The bending strength of CLST was lower than that of CLT from primary timber, while the bending stiffness was the same. In addition, the transverse vibration test approach was proven to be effective to estimate the stiffness of CLST without finger joints. Azeez [31] tested CLST panels made from mixed primary and secondary timber. The bending performance of the CLST samples was superior to that of the control CLT samples made of primary timber. Chulain et al. [32] tested CLST made from recovered spruce. The bending strength and stiffness were similar to that of CLT made of new spruce. These results suggest that production of CLST is a viable option for reuse of secondary timber. However, research on CLST is still quite limited. None of the previous full-scale tests for CLST panels included finger joints, which frequently would be used to extend the length of short pieces of secondary timber. In addition, most research has only used secondary timber as transverse layers, similar to fillers, so that the structural potential of secondary timber has not been fully investigated. Production of CLST entirely from secondary timber would be advantageous in scenarios where timber from urban demolition is available but primary timber from forestry is not available locally.

Although there have been studies to link the properties of feedstock materials with those of CLT products [33,34], the relationship between the properties of CLST and its base secondary materials has not been well-explored. Assessment of the structural properties of secondary timber and CLST is a challenge due to uncertainties such as a lack of information about the tree species and loading history. Research has begun to investigate non-destructive testing (NDT) of secondary timber, such as measurement of dynamic modulus of elasticity (dMoE) through stress waves [35,36], visual grading parameters [14,37], near-infrared spectroscopy [38], ultrasonic technology [39,40], scanning electron microscopy [41], and their combinations [42–44]. In addition, sonic tests [45], modal analysis [46,47], and vibration tests [30,48] have been used to predict the bending performance of CLT and CLST. Although such NDT methods have shown promise in predicting the results of destructive tests, the complicated associated analysis and need for access to costly facilities might restrict their application. The larger variability of secondary timber also requires collection of more data to rigorously validate and standardise the methods.

This paper thus presents an experimental investigation of critical properties of secondary timber for making CLST, and the CLST produced from it. Secondary timber was tested by economical NDT methods, and the results were compared with those from destructive tests. Then, 15 full-scale CLST specimens were manufactured entirely from finger-jointed secondary timber, and tested by NDT methods before loading to failure. Finally, an analytical model was proposed for the bending performance estimation of CLST, to provide design information for practising engineers.

2 Materials and methods

2.1 Materials

A total of 395 pieces of timber were collected. Among them, only four pieces were treated showing dark green colours and thus discarded at the preliminary process stage. Then the remaining 391 pieces of mixed species untreated softwood secondary timber were used in this investigation. Their lengths ranged from 750 mm to 3400 mm; their widths from 80 mm to 130 mm; and their thicknesses from 35 mm to 53 mm (Figure 1). The timber was deliberately collected from three different sources to simulate the real scenario of recovery of timber of unknown species and structural grades. 182 pieces were recovered joists and studs (Figure 2) from the top floor of a 1990s hotel in London. The grade stamps on some pieces indicated that they were originally likely to be C16 strength grade Chile Radiata Pine (*Pinus radiata*) [49,50]. 69 pieces were pine joists collected by DDS Reclamation Ltd. in Margate. The other 140 pieces were recovered by a timber recycling firm from joists and rafters of 19th- and early 20th-century houses in London. All batches were from previous indoor use, and were likely to have been exposed to a low-magnitude loading history, as is normal for roof and internal wall stud members [14]. The use of the three batches is shown in Figure 3 and will be further explained in following sections.

Assessment of the secondary timber started with a visual check when the materials first arrived at the structural lab on the University College London (UCL) Here East campus. This was followed by metal detection and removal before testing of stiffness and strength. Most joists were free of metals except for some long nails and notches at the ends (Figure 4a), which were therefore cut off with a chop saw. However, most studs contained dense small nails and screws at the ends and noggin positions (Figure 4b), which were manually removed by nail kickers and hammers.

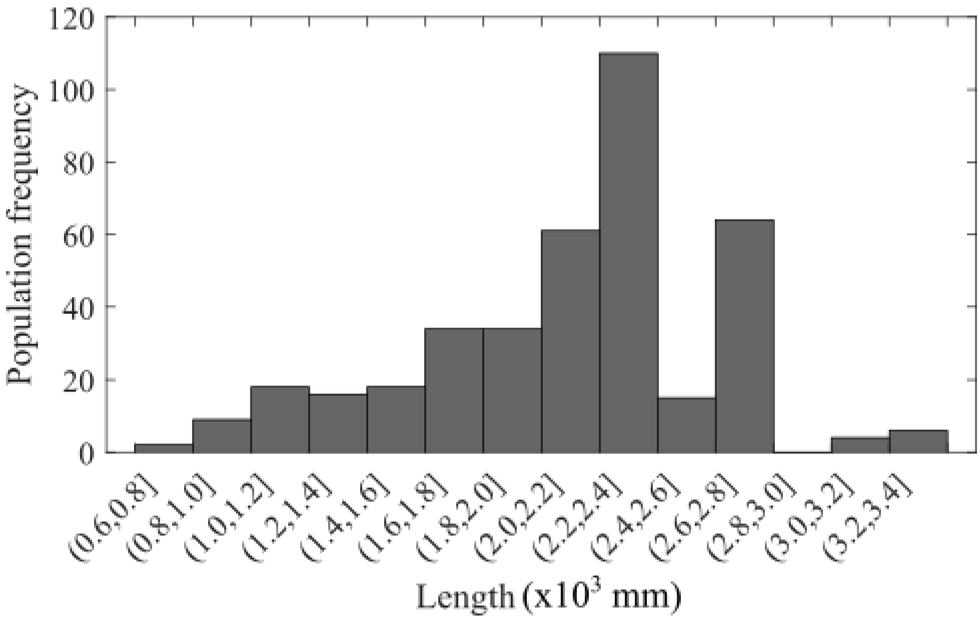
120
100
80
60
40
20
0
Population frequency
(0.6,0.8]
(0.8,1.0]
(1.0,1.2]
(1.2,1.4]
(1.4,1.6]
(1.6,1.8]
(1.8,2.0]
(2.0,2.2]
(2.2,2.4]
(2.4,2.6]
(2.6,2.8]
(2.8,3.0]
(3.0,3.2]
(3.2,3.4]
Length (x10^3 mm)

a)

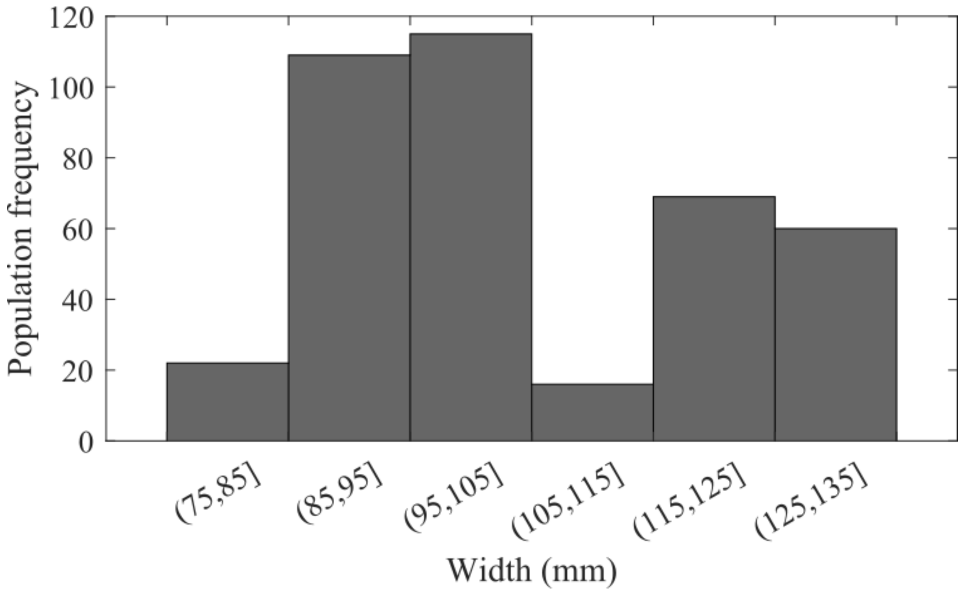
120
100
80
60
40
20
0
Population frequency
(75,85]
(85,95]
(95,105]
(105,115]
(115,125]
(125,135]
Width (mm)

b)

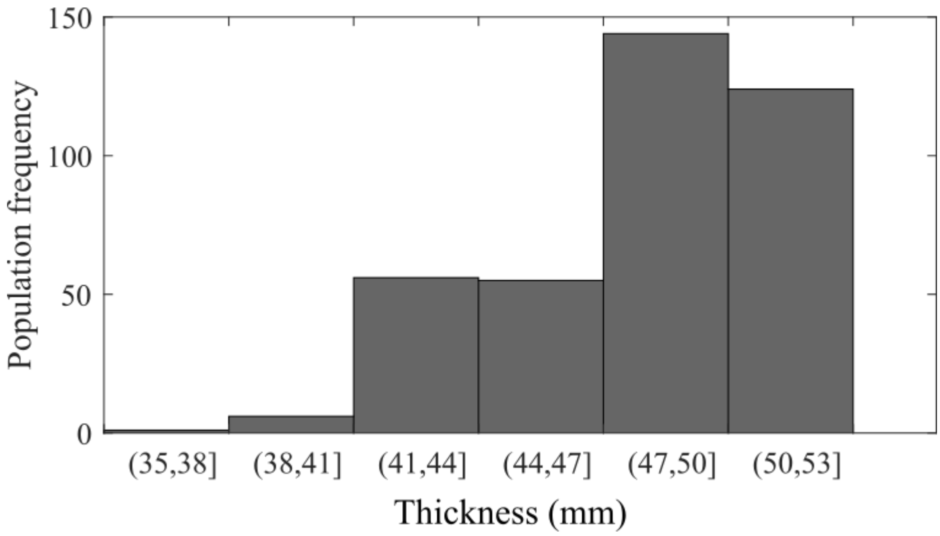

c)

Figure 1 Distributions of secondary timber piece lengths (a), widths (b) and thicknesses (c)

a) b)

Figure 2 Secondary timber pieces (b) from the demolition of the top floor of a hotel (a)

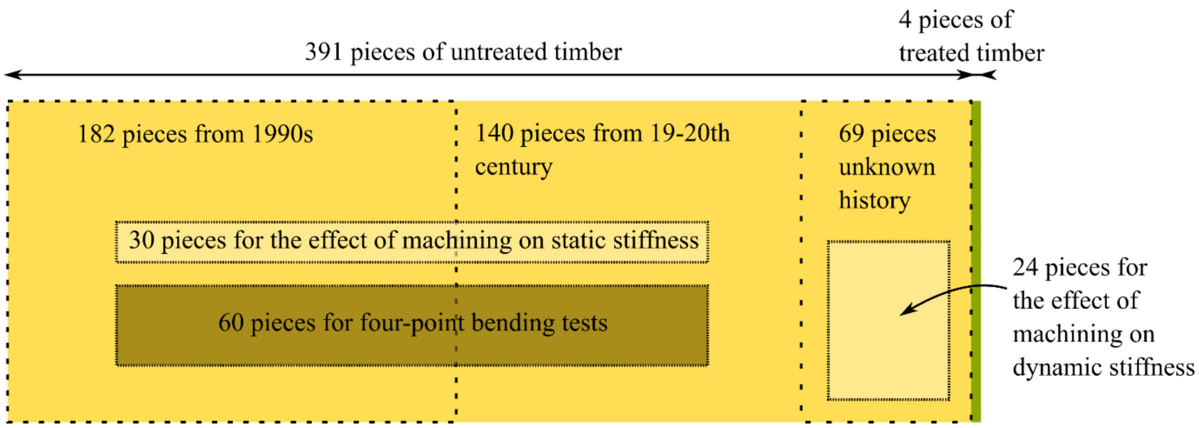

Figure 3 Use of secondary timber in this project

a) b)

Figure 4 Metal fixings in secondary timber joists (a) and studs (b)

2.2 Longitudinal vibration testing of secondary timber

An NDT method was used to determine the stiffness of secondary timber. After preliminary processing, the moisture content α of each piece was measured by a portable Brennenstuhl moisture detector. The mass and dimension of each piece were measured by a scale and tape measure, respectively. Then, longitudinal vibration tests were conducted for every piece of secondary timber by using a smartphone application, SmartThumper [51], developed by Mississippi State University. SmartThumper has been proven as a portable and economical tool for measuring dMoE when compared to other costly commercial devices [52,53]. The test setup is shown in Figure 5. The test piece spanned two foam pads as recommended by the instruction manual of SmartThumper [51]. A hammer was used to strike one end of the piece and a smartphone with SmartThumper installed was left on the same end to receive the longitudinal wave. More recommendations on the test setup can be found in the instruction manual of SmartThumper [51]. SmartThumper presented the peak frequency and corresponding dMoE directly by using Eq. 2.1a according to ASTM E1876-21 [54]. This dMoE obtained through a longitudinal vibration test, at moisture content α, was denoted as $dMoE_{L,\alpha}$. In addition, $dMoE_{L,\alpha}$ was adjusted to $dMoE_{L,12\%}$ at a reference moisture content of 12%, as suggested by EN 384 [55], using Eq. 2.1b from Evans et al. [56] that is recommended by SmartThumper manual [51]. Furthermore, longitudinal vibration tests were also conducted for 24 pieces of secondary timber before and after machining, to examine the influence of machining on dMoE. Another popular NDT method is the transverse vibration test. The longitudinal vibration test showed similar accuracy as the transverse vibration test for measuring dMoE [57]. Because SmartThumper is cost-effective and requires minimal facilities, only longitudinal vibration tests were conducted for the secondary timber.

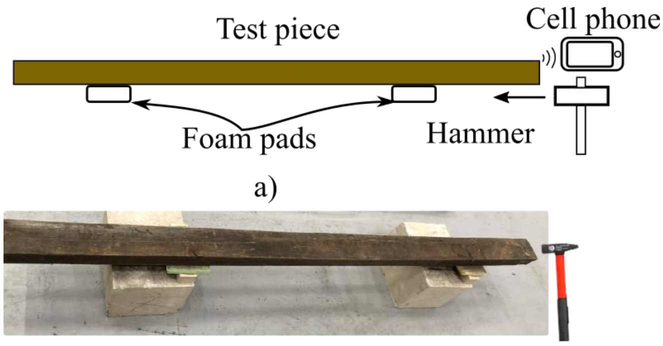

Figure 5 Longitudinal vibration test: sketch (a) and photograph (b) of test setup

$$dMoE_{L,\alpha} = \rho v^2 = \rho(2Lf_L)^2 \quad \text{Eq. 2.1a}$$

$$dMoE_{L,12\%} = \frac{(1.857 - 0.0237 \times 12)dMoE_{L,\alpha}}{(1.857 - 0.0237\alpha)} \quad \text{Eq. 2.1b}$$

where ρ is the timber density; L is the length of the test piece; and f_L is the first harmonic longitudinal vibration frequency.

2.3 Four-point bending tests for secondary timber

After the longitudinal vibration tests, four-point bending tests (flatwise) according to EN 408 [58] were conducted for 60 pieces of secondary timber (Figure 6) to validate the longitudinal vibration test method. All test pieces were long enough to span l=900 mm (not less than 18 times of thickness) and two loading points were 300 mm away from the closest support (i.e., a=300 mm in Figure 6). The loading speed was 8 mm/min. The middle span deflection was measured by linear variable differential transformers (LVDTs) and the global sMoE was calculated by Eq. 2.2 with an infinite shear modulus G, as suggested by EN 408 [58]. Local sMoE was not measured because other research showed that local sMoE of secondary timber was difficult to obtain accurately due to the initial specimen twist [59]. 60 pieces of secondary timber were tested for sMoE without machining because they contained fractured nails and screws that could not be withdrawn. These 60 pieces were then loaded until failure to calculate the MoR of secondary timber $f_{m,st}$, as per Eq. 2.3. In addition, 30 pieces of secondary timber were machined to regular sizes and only tested elastically to obtain their sMoE, which was compared with sMoE of unmachined pieces to estimate the influence of machining on the stiffness.

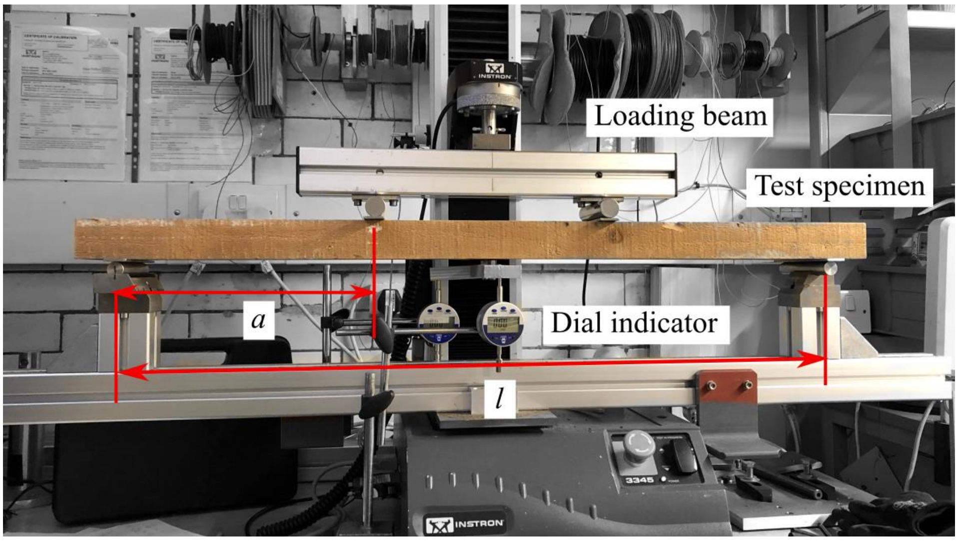

Figure 6 Bending tests setup according to EN 408 [58]

$$sMoE_g = \frac{3al^2 - 4a^3}{2bh^3\left(2\frac{w_2 - w_1}{F_2 - F_1} - \frac{6a}{5Gbh}\right)} \qquad \text{Eq. 2.2}$$

$$f_{m.st} = \frac{3F_m a}{bh^2} \qquad \text{Eq. 2.3}$$

where $sMoE_g$ is the global static MoE; a is the distance between the loading point and its closest support as shown in Figure 6; l is the span of the specimen; b and h are the cross-sectional width and height of the test piece; F_2 and F_1 are 40% and 10% of the estimated maximum load F_m, respectively; w_2 and w_1 are the corresponding middle span displacement; and G is the shear modulus.

2.4 Manufacturing of CLST

Fifteen three-layer CLST panels were manufactured in the structural lab at UCL. All panels for testing had a final dimension of 2550 mm x 320 mm x 102 mm and all layers were made from secondary timber. Figure 7 shows the process of CLST manufacturing in the lab. Firstly, visible metals were removed manually by the nail kickers and hammers during the preliminary process. Secondly, all timber pieces were scanned by an industry-level metal detector to ensure they were clear of metal contaminants. Thirdly, those timber parts that contained invisible metals or metals that could not be withdrawn easily were cut off by a chop saw and discarded (e.g., piece No.2 in Figure 7). The remaining parts (e.g., pieces No.1 and No.3 in Figure 7) were passed through the metal detector again to guarantee that they contained no metals. Fourthly, clean timber pieces were machined to regular sizes by a planer and thicknesser to get rid of the decayed surfaces and deformation. Although the aged surfaces of timber pieces shorter than

1.2 m could usually be removed by 2 mm planing, which got rid of the timber's dark brown colour aged surface and exposed its true yellow colour, surface twist deformation required more material to be removed for timber pieces longer than 1.6 m. All pieces were machined to a consistent thickness of 34 mm to take full advantage of the majority of lengths that were longer than 1.6 m and those pieces that were thinner than 41 mm (Figure 1). The CLST outer layers were made of lamellae with both 110 mm x 34 mm and 75 mm x 34 mm cross sections; the middle layers were made of lamellae with a 90 mm x 34 mm cross-section. Fifthly, timber pieces shorter than 2.55 m were finger jointed to a length of 2.55 m. Among the 391 pieces, only 27 pieces longer than 2.55 m remained after chopping and were directly used as outer layers. The rest were jointed to the desired length through structural finger joints at Inwood Development Ltd., a glulam manufacturer near London. Sixthly, all panels were glued by two-component melamine urea-formaldehyde (MUF) adhesive (Prefere 4535 and Prefere 5035) supplied by Dynea. Emission of toxic chemicals (e.g., formaldehyde) from this adhesive met indoor-use requirements without a special extraction system. The adhesive was applied at a spread rate of 150-250 g/m^2 as per the product's technical sheet. Seventhly, the panels were pressed by a vacuum press for eight hours at a room temperature of 16 °C until the adhesive was fully cured. Finally, the panels were cut by a vertical band saw to the target dimension.

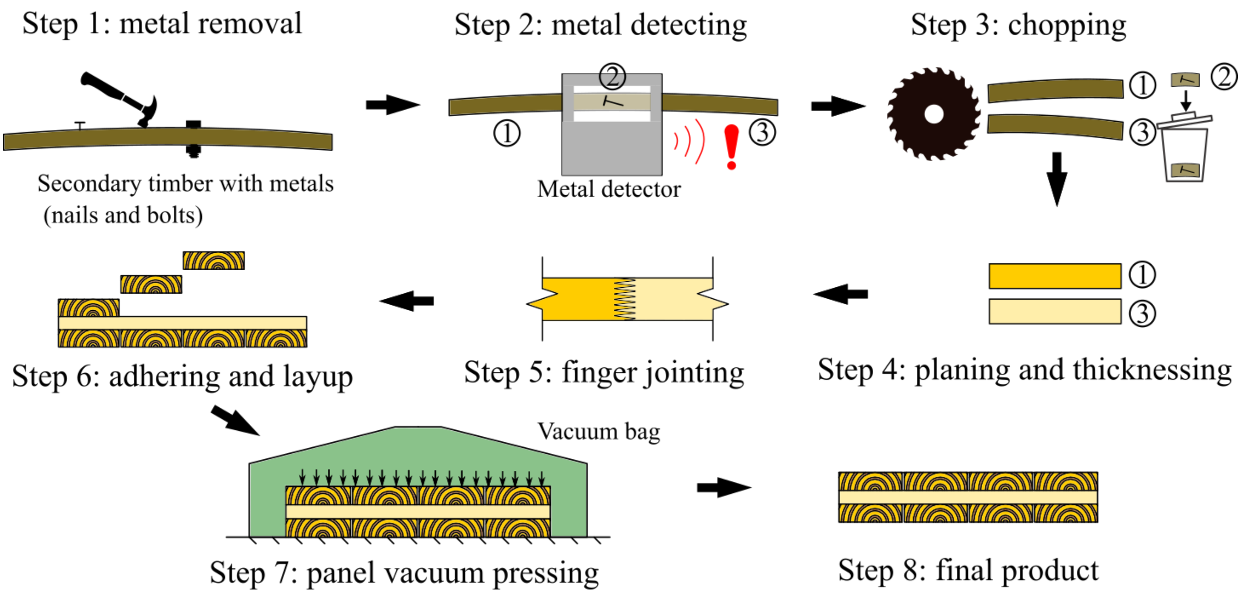

Figure 7 CLST manufacturing process in the lab

2.5 Transverse vibration tests for CLST

Transverse vibration tests were conducted to assess the stiffness of the CLST panels because past research [30] has shown that transverse vibration tests provide a better prediction of CLST stiffness than longitudinal vibration tests. Testing was conducted according to ASTM D6874-21 [60] because the CLST panels were considered as beam-like samples according to Zhang et al. [61]. The panels were simply supported on two supports as shown in Figure 8 with 25 mm overhanging on each side of the support. An accelerometer was attached to the middle span of the panel and the centre of the panel was hit by a hammer. The transverse vibration frequency was captured by the accelerometer to calculate the dMoE of the CLST panels by Eq. 2.4.

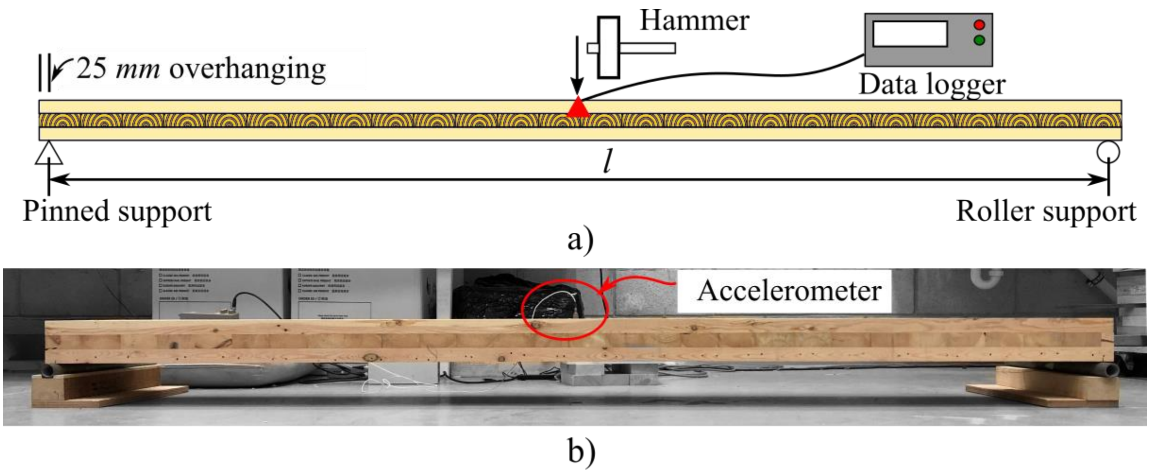

Figure 8 Flexural vibration tests of CLST panels: sketch (a) and photograph (b) of test setup

$$dMoE_{CL,T} = \frac{f_T^2 W l^3}{K_d I_{CL,net} g(\frac{l_t}{l})} \qquad \text{Eq. 2.4}$$

where $dMoE_{CL,T}$ is the dMoE of CLST panel through transverse vibration tests; f_T is the fundamental transverse vibration frequency; W is the weight of the CLST panel; l=2500 mm is the span of the CLST panel; K_d =2.47 for the simply supported condition; $I_{CL,net}$ is the moment of inertia calculated from properties of the layers having its fibres parallel to span only; l_t = 2550 mm is the total length of the specimen.

2.6 Four-point bending tests for CLST

Four-point bending tests, similar to those described in Section 2.3, were conducted for the 15 CLST panels according to BS EN 16351 [62] in the Strengths of Materials laboratory at London South Bank University. The test setup is shown in Figure 9a. The distance between the two loading points was 6h_c and the distance between the loading point and its closest support was increased to 9h_c to facilitate triggering the bending failure. The loading speed was 6 mm/min. Each specimen was equipped with eight LVDTs as shown in Figure 9b. LVDT1 and LVDT2 were installed at the top of both edges of the middle span to measure the middle span deflection; LVDT3 and LVDT4 were installed at the neutral axis of both edges of the middle span to measure the local deflection between the gauge length (i.e., the middle $5h_c$); LVDT5 to LVDT8 were installed at the top of both edges of the support position to monitor the indentation deformation at the supports. The bending stiffness was determined by Eq. 2.5 according to EN 16351 [62].

$$sMoE_{CL} = \frac{l_2 l_1^2}{16 I_{CL,net}} \frac{F_2 - F_1}{w_2 - w_1} \qquad \text{Eq. 2.5}$$

where $sMoE_{CL}$ is the sMoE of the CLST panel; l_2 is the distance between the loading point and its closest support (Figure 9b); l_1 is the gauge length (Figure 9b); F_2 and F_1 are 40% and 10% of the estimated maximum load F_m, respectively, and w_2 and w_1 are the corresponding deformations that were calculated by the average value of LVDT3 and LVDT4.

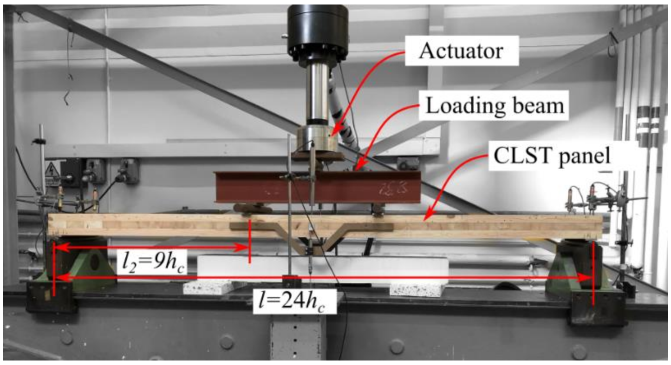

a)

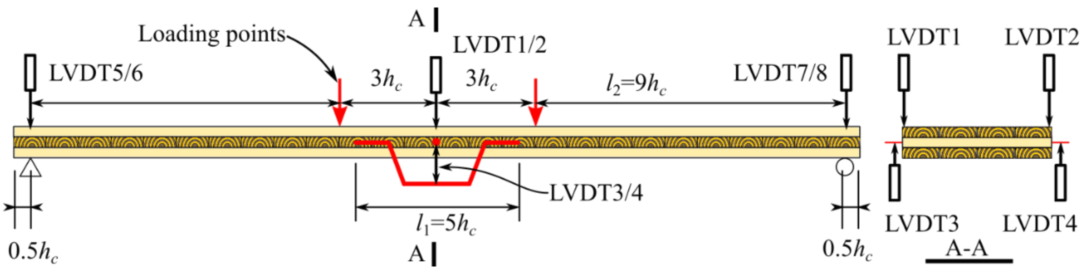

b)

Figure 9 Test setup (a) and LVDT configurations (b) for four-point bending tests of CLST

All specimens were further loaded until failure to calculate the MoR. Because EN 16351 [62] does not explicitly include an equation to calculate the MoR of CLT, two equations from different standards were used. Eq. 2.6 was recommended by Corpataux et al. [63] as per Eurocode 5 [64] while Eq. 2.7 in ASTM D198 [65] and EN 408 [58] was recommended by US standard PRG 320 [28] and Pang et al. [66].

$$f_{m,CL,EU} = \frac{F_m l_2}{2 I_{CL,net}} z_s \qquad \text{Eq. 2.6}$$

$$f_{m,CL,US} = \frac{3F_m l_2}{b_c h_c^2} \quad \text{Eq. 2.7}$$

where $f_{m,CL,EU}$ and $f_{m,CL,US}$ are MoR of CLST panels according to Eurocode 5 [64] and PRG 320 [28]; z_s is the distance between the edge of CLST to the neutral axis; b_c and h_c are the cross-section width and height of the CLST panel; F_m is the maximum load.

2.7 Analytical models

Analytical models can be useful for predicting material structural properties for practising engineers because experimental tests are costly and cannot be exhaustive. Therefore, the stiffness and strength results from experimental tests were compared with the two widely-used analytical models in the Canadian CLT handbook [67], i.e., γ-method and shear analogy (SA) method, to evaluate the effectiveness of these two analytical methods. These two methods use the sMoE and bending strength of the constituent timber to calculate the strength and stiffness of CLT. The effective bending stiffnesses $(EI)_{eff}$ calculated by the two methods were denoted as $(EI)_{eff,gamma}$ and $(EI)_{eff,SA}$, respectively, as shown in Eq. 2.8 and Eq. 2.9. The moment capacity of the CLST panels was calculated by Eq. 2.10 and Eq. 2.11 using the two methods as well. It is noted that the strength modification factor K_{rb}=0.85 for the SA method in CLT handbook was not included in Eq. 2.11 as this is an empirical factor for conservative estimates based on test observations of CLT.

$$(EI)_{eff,gamma} = \sum_i (E_i b_i h_i^3/12) + \sum_i (\gamma_i E_i b_i h_i z_i^2) \quad \text{Eq. 2.8a}$$

$$\gamma_i = \left(1 + \frac{\pi^2 E_i b_i h_i h_j}{l^2 G_{90,j} b_j}\right) \quad \text{Eq. 2.8b}$$

$$G_{90,j} = 30 + 17.5\alpha_{bt,j} \quad \text{Eq. 2.8c}$$

$$(EI)_{eff,SA} = \sum_i (E_i b_i h_i^3/12) + \sum_i (E_i b_i h_i z_i^2) + \sum_j \left(E_{j,90} b_j h_j^3/12\right) + \sum_j \left(E_{j,90} b_j h_j z_j^2\right) \quad \text{Eq. 2.9}$$

$$M_{gamma} = f_{m,CLT,k} \frac{(EI)_{eff,gamma}}{E_{mean}(\gamma_i z_1 + 0.5h_1)} \quad \text{Eq. 2.10}$$

$$M_{SA} = f_{m,CLT,k} \frac{(EI)_{eff,SA}}{E_{mean}} \frac{2}{h_{CL}} \quad \text{Eq. 2.11}$$

where E_i is the MoE of sawn timber in the major direction; b_i, h_i are the width and height of the i-th layer in the major direction; z_i is the distance from the centroid of the i-th layer to the centroid of the cross-section; γ_i is the connection efficiency factor for the i-th layer; b_j, h_j are the width and height of the j-th layer in the minor direction; l is the span of the CLST panel;

$E_{j,90}$ is the MoE perpendicular to grain for the j-th layer in the minor direction and is assumed to be 1/30 of the MoE parallel to grain, based on EN 338 [49]; z_j is the distance from the centroid of the j-th layer to the centroid of the cross-section; $\alpha_{bt,j}$ is the aspect ratio of the j-th layer in the minor direction; $G_{90,j}$ is the rolling shear stiffness of the j-th layer in the minor direction and is calculated by Eq. 2.8c according to Ehrhart et al. [68]; E_{mean} is the average MoE in the outermost layer; $f_{m,CLT,k}$ is the characteristic bending strength of CLT.

3 Results and discussion

3.1 Yield of secondary timber through manufacturing

Among the 391 untreated pieces of timber, 60 pieces were kept for destructive tests. The remaining 331 pieces had a total length of 758.3 m. After metal removal and machining in steps 1-4 (Figure 7), a total length of 589.6 m was retained and machined to a thickness of 34 mm: a length yield of 77%. In step 5, the finger jointing consumed a further 9% of the total length. During steps 1-5, it became apparent that recovered joists are more desirable raw materials for CLST than studs based on the following observations: 1) Joists usually had a bigger cross-section size than studs, providing more tolerances for machining and a higher aspect ratio for middle layers; 2) Joists contained fewer metal contaminants, which significantly boosted the metal removal speed (35 m/hour for joists versus 15 m/hour for studs); 3) The studs containing small nails sometimes left metal particles from their screw- or ring-shanks after metal removal, which would still trigger the metal detector and cause rejections; 4) The chopping in step 3 left some unusable studs shorter than 0.4 m, the minimum length for finger-jointing, which were also discarded. As a result, the length yield from studs was 60.5% whereas the yield from joists was 93.0%.

3.2 Comparison between dMoE and sMoE of secondary timber

The sMoE of the 60 secondary timber pieces tested by four-point bending tests according to EN 408 [58] are plotted against the dMoE values obtained from the longitudinal vibration test in Figure 10. 18 of these pieces were from 19th- and early 20th-century houses with a nominal dimension of 75 mm x 50 mm and denoted as Batch 1; 20 pieces were from 19th- and early 20th-century houses with a nominal dimension of 100 mm x 50 mm and denoted as Batch 2; 22 pieces were from the 1990s hotel with a nominal dimension of 100 mm x 50 mm and denoted as Batch 3. Least squares regression of sMoE as a function of dMoE, was conducted because previous research demonstrated a linear relationship between these variables [69]. The slopes

(β_1) and intercepts (β_0) are listed in Table 3.1. The slopes (β_1) of the separate regression lines for the three batches with different nominal dimensions and ages were similar, ranging from 0.64 to 0.68. Batch 1 and Batch 2 were of similar ages but had different nominal dimensions. Batch 2 and Batch 3 had the same nominal dimensions but were from different ages. To compare the effect of cross-sections and ages, analysis of variance (ANOVA) was conducted for sMoE of Batch 1 and Batch 2 and sMoE of Batch 2 and Batch 3 (listed in Table 3.2). The null hypothesis is that the cross-sections/ages have no significant difference in the sMoE results. The p-values for them are 0.362 and 0.152, respectively, which is higher than the assumed significance level (0.05). This verified that the age of the timber and deviation of nominal dimensions did not cause major differences in bending stiffness for timber pieces that had been well protected in an indoor use environment under normal loading conditions. Other research has also shown that there was no difference in MoE for slightly larger 2x4", 2x8" and 2x10" nominal cross-section timber [70] and ASTM 1990-19 [71] does not consider an effect of cross-section in determination of MoE. Therefore, it seems feasible to combine different sources of secondary timber during structural property assessment, which is of practical importance for recycling, since secondary timber will commonly be sourced from different buildings (e.g., multiple houses) to accumulate a useful volume. The analysis in the following sections combines the results of all batches without considering differences in timber ages and cross-sections.

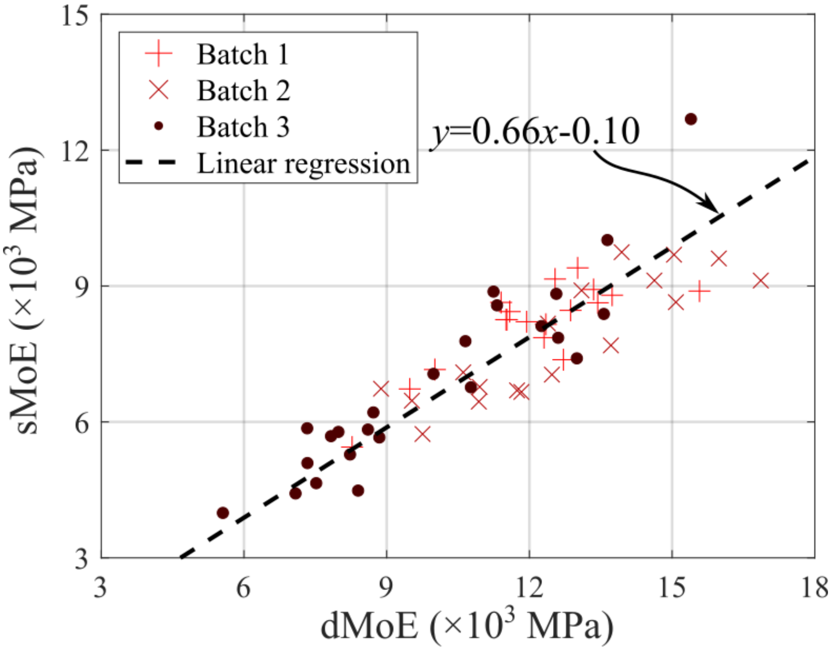

Figure 10 Comparison between dMoE determined by longitudinal vibration testing and sMoE determined by four-point bending testing for unmachined secondary timber

Table 3.1 Linear regression coefficients between sMoE and dMoE

Batch No.	Mean *dMoE* (MPa)	Mean *sMoE* (MPa)	Intercept β_0	Slope β_1	Coefficient of determination r^2
1	12090	8150	-0.12	0.68	0.50
2	12640	7800	-0.42	0.64	0.68
3	9770	6940	0.11	0.68	0.85
Combined batch 1-3	11610	8140	-0.10	0.66	0.75
4	11970	9350	0.54	0.73	0.85

Table 3.2 ANOVA result for sMoE of secondary timber

Group	F-value	p-value
Batch 1 and Batch 2	0.85	0.362
Batch 2 and Batch 3	2.14	0.152

Although sMoE and dMoE were found to be correlated for secondary timber, the sMoE was a lower proportion of the dMoE than in past research, such as 0.73-0.80 obtained by Yang et al. [69]. It was postulated that the difference could be attributable to use of unmachined timber in our experiments. To investigate the influence of machining, 30 pieces of secondary timber were selected with a mixture of ages and cross-sections from the remaining 331 pieces and machined to a regular cross-section (denoted as Batch 4). The resulting sMoE and dMoE values are plotted in Figure 11, with the equation for the associated regression line. The slope was increased to 0.73 after machining. The reason could be that the cupping deformation of secondary timber caused some gaps at the support, and thus reduced the compression area perpendicular to grain as shown in Figure 12, so the global deflection was larger. Arguably, a slope of 0.73 should be used to represent the relationship between sMoE and dMoE because all pieces are machined when manufacturing CLST panels.

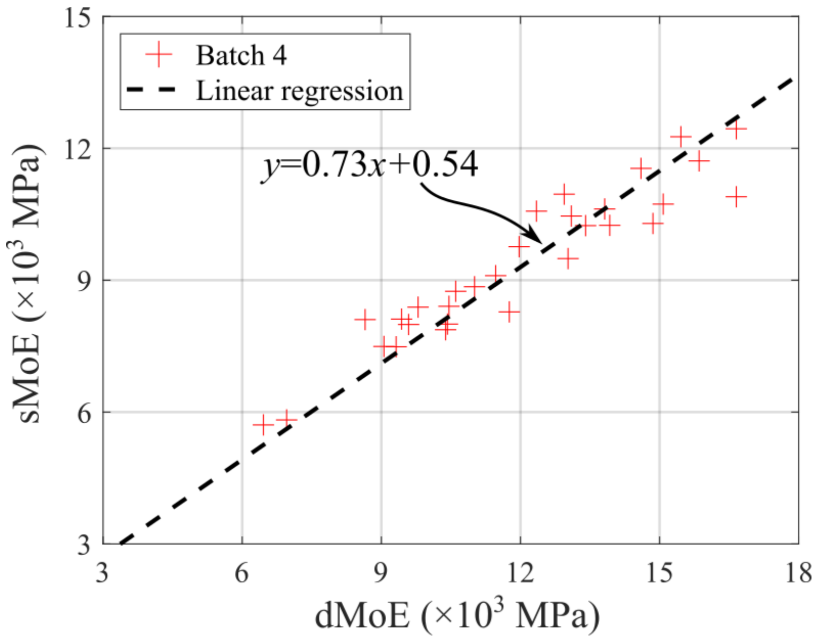

Figure 11 Comparison between dMoE and sMoE for machined secondary timber

a) b)

Figure 12 Cupping of secondary timber (a), and resulting gap during testing (b)

For the 30 pieces of machined secondary timber, dMoE was obtained before machining (steps 3-4 Figure 7) because the non-destructive longitudinal vibration tests were expected to become less accurate when the length became shorter [51]. However, EN 14081-1 [72] requires that structural timber shall be re-graded if the reduction in dimension is greater than 5 mm and 10 mm for 22 mm-100 mm dimension and more than 100 mm dimension, respectively. The reduction limit could commonly be exceeded during the processing of secondary timber. To investigate the effect of the change of dimension through machining, the dMoE of 24 pieces of secondary timber longer than 2.55 m was compared before and after machining as shown in Figure 13. The results showed that the average dMoE after machining was 1.5% lower than that before machining. The maximum difference between the dMoEs was -10.5% even for a dimension change greater than 10 mm. Therefore, the dMoE before machining was practically equivalent to that after machining: a useful finding for a notional CLST producer, as it enables preliminary categorisation of secondary timber pieces according to their dMoE, without wasting time and energy in removing metal fixings and machining of substandard pieces.

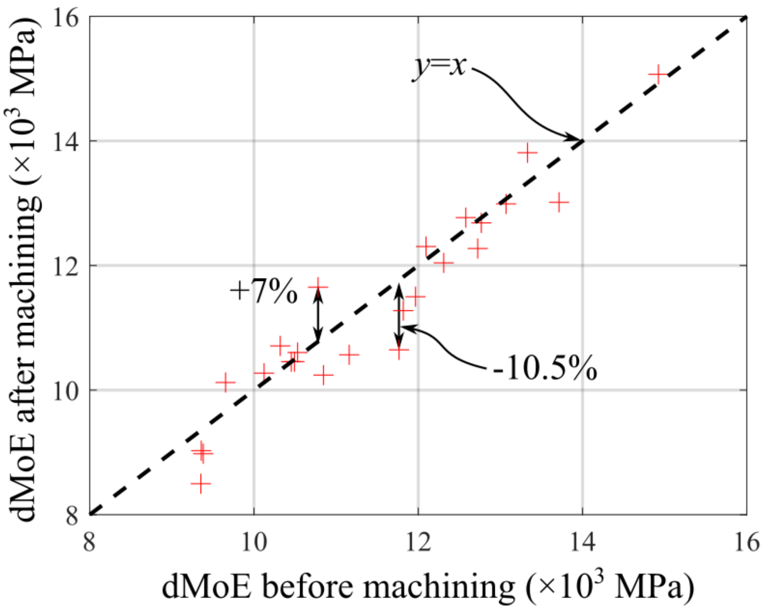

Figure 13 Comparison of dMoE before and after machining

3.3 Comparison between MoE and MoR of secondary timber

The 60 secondary timber pieces were tested to failure under the four-point bending test setup according to EN 408 [58] after measuring their sMoE. The failure mode was bending failure at the tension side mostly due to the existence of knots (Figure 14). Table 3.3 shows that the MoR had a much higher coefficient of variation (CoV) than the MoE, as also found in past research for primary timber [73]. The higher CoV is due to the fact that MoR is usually governed by a local defect (such as knots as shown from tests) while MoE presents a global property of a whole piece. As a result, the coefficients of determination were low between MoR and sMoE (r^2 = 0.33) and between MoR and dMoE (r^2 = 0.23).

Figure 14 Bending failure of secondary timber

Table 3.3 dMoE, sMoE and MoR of secondary timber

Item	Mean (MPa)	CoV (%)	Characteristic value (MPa)
dMoE	11430	22	11200
sMoE	7540	22	7390
MoR	32.7	46	15.1

The characteristic values of bending strength (i.e. MoR), sMoE and dMoE were calculated according to EN 14358 [74]. The characteristic mean value of dMoE was 11200 MPa. By using the linear equation in Figure 10, the predicted characteristic mean value of sMoE was 7290 MPa, close to the calculated sMoE of 7390 MPa. If the linear equation in Figure 11 were used, taking into account the positive effects of machining, the predicted mean value of sMoE (8720 MPa) would be stiffer than the specified MoE (8000 MPa) for the C16 grade in EN 338 [49]. The characteristic MoR was 15.1 MPa, greater than the specified strength $f_{m,st}$=14 MPa for the C14 grade in EN 338 [49]. Given the C16 stamps on some timber pieces, a bending strength consistent with C14 suggests that secondary timber might experience a slight strength degradation due to its previous service, although there is no stiffness degradation. This observation is consistent with findings summarized by Cavalli et al. [12].

Because dMoE did not provide a good prediction of MoR, a method similar to that described by Crews and Mackenzie [14] was proposed here to assign MoR for secondary timber. Hypothetically, if non-destructive dMoE measurement is used to predict sMoE, the corresponding grade for this sMoE in EN 338 [49] (i.e., C16) should be reduced by one grade (i.e., C14) to take into account the potential strength degradation. Longitudinal vibration tests and tensile tests for secondary timber conducted for secondary timber by Huang [75] were used to validate this proposed property estimate. The characteristic mean dMoE based on her tests was 8980 MPa. This dMoE was used to calculate the characteristic mean sMoE of 7090 MPa by the regression equation from Figure 11, which was higher than the specified value for the

C14 grade (7000 MPa). The tensile tests resulted in a characteristic tensile strength of 7.7 MPa, which was slightly lower than the specified value (8 MPa) for the C14 grade, so the method was also applicable to Huang's test data [75]. However, it should be noted that the properties in EN 338 [49] were only used for grade estimation because current knowledge is not sufficient to build a grade table for secondary timber. The quantification of these and other strength grades and structural properties requires further verification.

3.4 Comparison between dMoE and sMoE of CLST

Transverse vibration tests were conducted for 15 CLST panels. The dMoE values from transverse vibration tests calculated by Eq. 2.4 ($dMoE_{CL,T}$) were compared with $sMoE_{CL}$ values calculated by Eq. 2.5 (Figure 15). The $dMoE_{CL,T}$ for the first CLST panel that was manufactured in the lab, which deformed after curing due to moisture change, was significantly offset from other data points and thus was removed from the linear regression. The deformation prevented full contact of the panel with the support (Figure 16). Figure 15 illustrates that it was possible to use the $dMoE_{CL,T}$ to predict $sMoE_{CL}$ but the r^2 was low (0.39) when compared with past research (such as r^2=0.85 from Llana et al. [30]). Past research showed that cracks could influence the vibration frequency [61], so the reason for the difference could be the existence of more cracks and finger joints in CLST panels, which reduced the vibration frequency. Further verification might be required to quantify this influence, for example, by comparing CLST panels with and without finger joints.

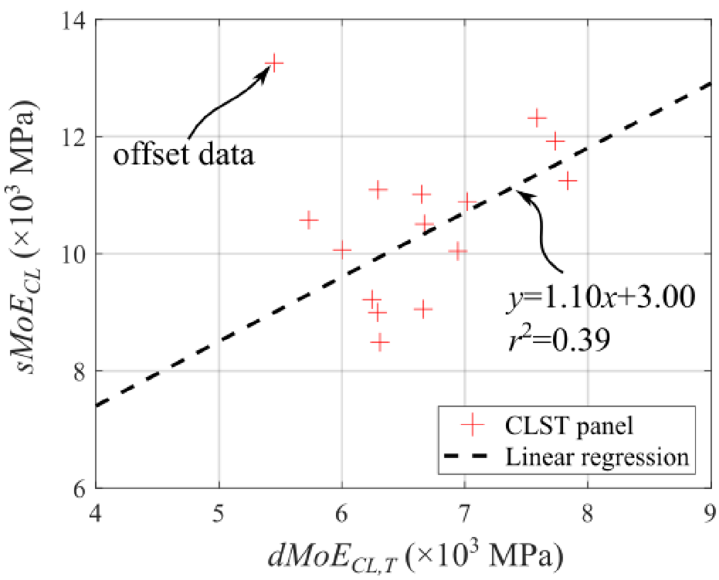

Figure 15 Comparison between $dMoE_{CL,T}$ and $sMoE_{CL}$

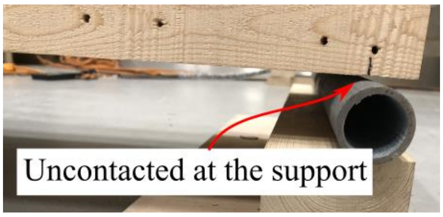

Figure 16 CLST surface that was not in full contact with the support

Past research has illustrated that the bending stiffness of a CLT panel is highly related to the stiffness of the timber in its major direction, i.e., the outer two layers of the three-layer product [67,76]. The $sMoE_{CL}$ for the panels was therefore compared with the average dMoE of the secondary timber pieces (Section 2.2) used in the major direction of the panels (Figure 17). The average value of dMoE showed a good linear relationship with $sMoE_{CL}$. Therefore, the average dMoE of the secondary timber pieces in the major direction was more useful for predicting $sMoE_{CL}$ than $dMoE_{CL,T}$ from transverse vibration tests. These results provide a straightforward approach to assessing the bending stiffness of CLST panels from the properties of their component materials. Measuring dMoE of secondary timber should thus be done before CLST manufacturing, also for quality control of the feedstock. This information can then be used to calculate sMoE of the final product, such that measurement of the dMoE of CLST panels themselves is not required, which would be more efficient and cost-effective, especially for larger CLST panels.

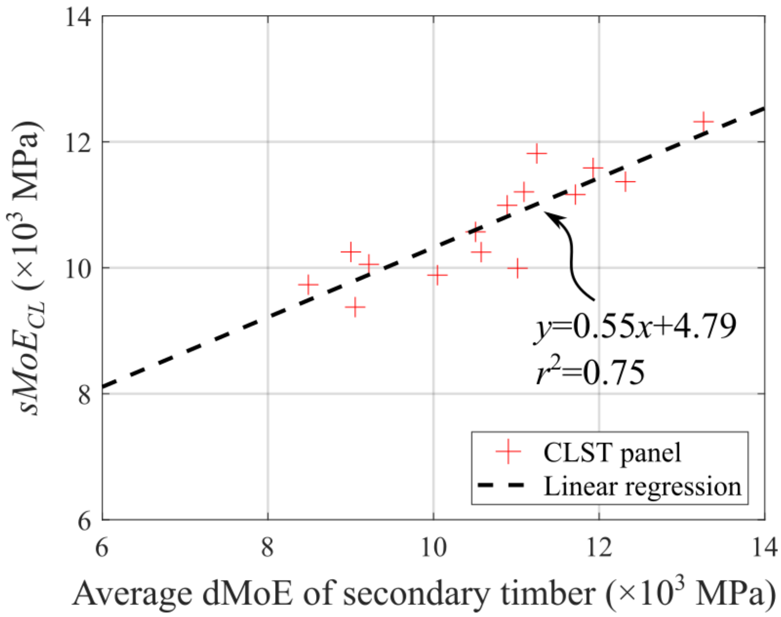

Figure 17 Comparison between average dMoE of secondary timber pieces in the major direction of a CLST panel and $sMoE_{CL}$ of the whole CLST panel

3.5 Comparison between MoE and MoR of CLST

The 15 CLST panels were tested until failure. The load-displacement curves are shown in Figure 18. The failure mode was bending failure between two loading points mostly due to the existence of knots (Figure 19a). Some panels also experienced delamination followed by bending failure (Figure 19b). It was noted that none of the panels failed at the finger joints. Therefore, finger joints did not have a noticeable influence on the bending strength for CLST panels made of relatively low-strength secondary timber.

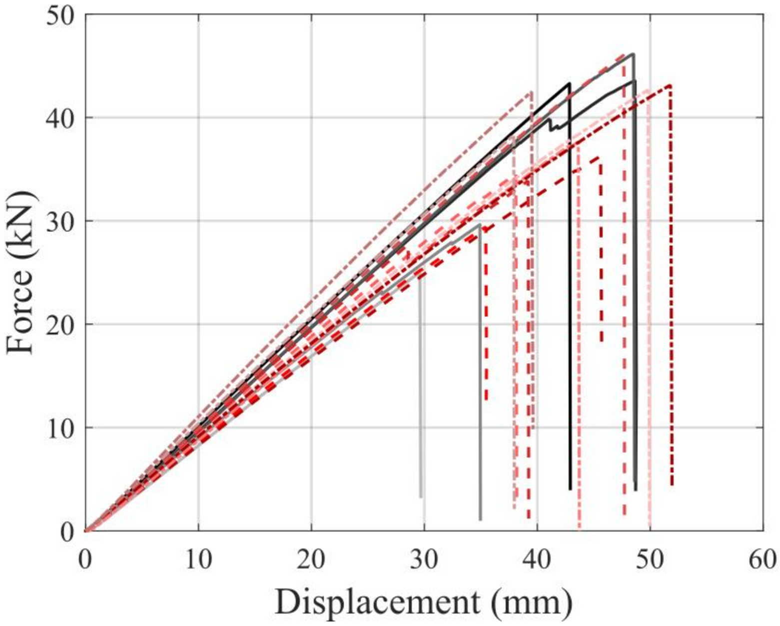

Figure 18 Force-displacement curve of CLST panels

a) b)

Figure 19 Failure mode of CLST panels (a) Bending failure (b) Delamination with bending failure

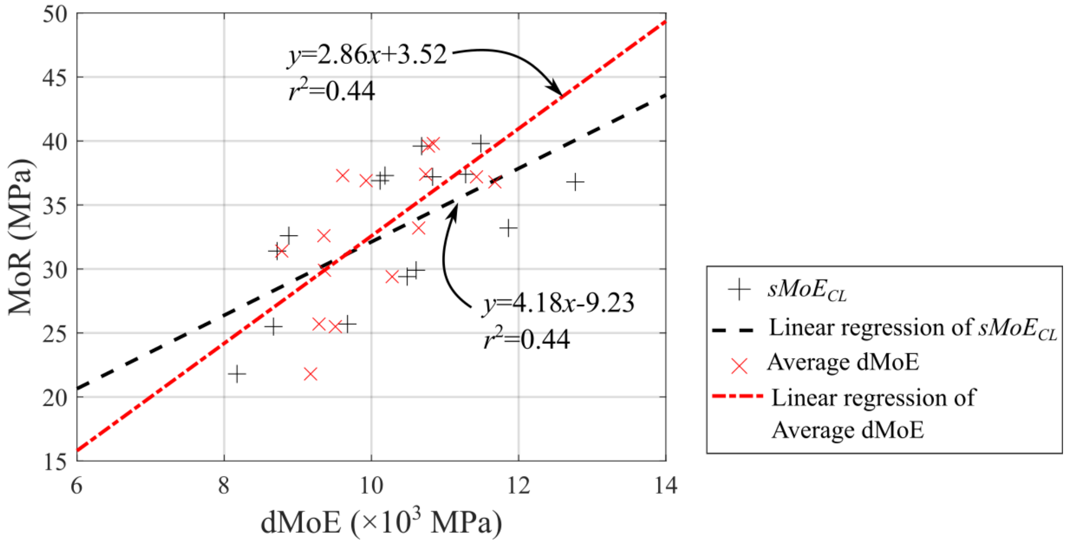

Figure 20 Comparison between MoE values of secondary timber pieces or of whole panel, and MoR values for CLST panels

Figure 20 compares the MoR of each CLST panel with its $sMoE_{CL}$ and the average dMoE of secondary timber pieces used in the major direction of the panel. While r^2 for MoR of CLST and $sMoE_{CL}$ or average dMoE were similar and both low (0.44), r^2 between MoR and MoE for CLST were higher than that between MoR and MoE of secondary timber (0.33 for MoR and sMoE and 0.23 for MoR and dMoE as mentioned in Section 3.3), probably due to the homogenisation effect of laminated timber products. The characteristic mean $sMoE_{CL}$ and 5-percentile MoR calculated as per Eq. 2.6-2.7 and EN 14358 [74] are listed in Table 3.4. Table 3.4 shows that the CoVs of the $sMoE_{CL}$ (13%) and MoR (17%) for CLST were much lower than those for secondary timber in Table 3.3 (22% for sMoE and 46% for MoR), illustrating that the homogenisation effect significantly reduced the variability of the properties of the constituent timber. Although CLT grades are still not specified in European standards, Unterwieser and Schickhofer [34] proposed a CL 24h grade (for CLT made of T14 grade Norway Spruce), with a specified bending strength $f_{m,EU}$ of 24 MPa and sMoE of 11600 MPa. The test results of the CLST panels were slightly lower than the CL24h specification (5% lower for $f_{m,EU}$ and 13% lower for sMoE), but this is attributable to use of T8 grade (equivalent) secondary timber, rather T14 Norway Spruce. The $sMoE_{CL}$ and $f_{m,US}$ of our CLST panels fell within the E3 CLT grade ($sMoE_{CL}$ =8300 MPa and $f_{m,US}$ =17.4 MPa) of ANSI/APA PRG-320 [28], applicable in the USA. This suggests that the properties of CLST panels are comparable to those of standard CLT products and are suitable for structural use of CLST in buildings.

Table 3.4 $sMoE_{CL}$, maximum strength and calculated bending strength for CLST panels

No.	$sMoE_{CL}$ (MPa)	F_{max} (kN)	$f_{m,CL,EU}$ (MPa)	$f_{m,CL,US}$ (MPa)
P1	10830	43.60	37.2	35.8
P2	11280	43.84	37.4	36.0
P3	10680	46.43	39.6	38.2
P4	9680	29.95	25.7	24.8
P5	8170	25.34	21.8	21.0
P6	8700	29.72	25.5	24.6
P7	10610	34.86	29.9	28.8
P8	8720	36.59	31.4	30.3
P9	10490	34.18	29.4	28.3
P10	11490	46.35	39.8	38.3
P11	10120	42.97	36.9	35.5
P12	8880	37.97	32.6	31.4
P13	10180	43.44	37.3	35.9
P14	11860	38.61	33.2	31.9
P15	12770	42.80	36.8	35.4
Characteristic value	10050	26.42	22.7	21.9
COV (%)	13%	17%	17%	17%

3.6 Comparison between test results and analytical models

The analytical models were compared with the test results. The average dMoE of secondary timber in its major direction was converted to sMoE by the linear equation in Figure 11. The sMoE was used to represent E_i in the outer layer for Eq. 2.8 and Eq. 2.9. The characteristic values of $(EI)_{eff}$ from the 15 CLST panels are listed in Table 3.5 as well as the characteristic values for moment capacity.

Table 3.5 shows that both analytical methods provided conservative estimates for $(EI)_{eff}$. Based on the assumption that the secondary timber grading was equivalent to C14, the moment capacity was 41% and 38% lower than the test result. The underestimate was due to the ignorance of the positive effects of laminating timber in engineered products [34]. A bearing model that was proposed for glulam [77] and then extended to CLT [78] was therefore used to account for the laminating benefits. The bearing model links the characteristic tensile strength parallel to the grain of the constituent timber, $f_{t,0,k}$, to the characteristic bending strength of CLT, $f_{m,CLT,k}$, as shown in Eq. 3.1. The bearing model for CLT is used here for CLST as well. $f_{t,0,k}$=8 MPa was used to calculate $f_{m,CLT,k}$, because the sMoE and MoR test results in Section 3.3 showed that our secondary timber was stronger than the T8 strength grade in EN 338 [49]. It is also noted that $k_{cov,t}$ of the bearing model (Eq. 3.1d) is an adjustment factor that reflected the gain from homogenisation of the properties of secondary timber with a higher variability [17].

By accounting for the effect of lamination using the bearing model, $f_{m,CLT,k}$ was increased from 14.0 MPa to 20.5 MPa, so the corresponding bending moment capacity was much closer to the experimental test values (Table 3.5). However, it should be noted that the bearing model was developed for CLT with homogeneous Norway Spruce as the constituent timber. The factors used here might need further refinement as the availability of test data for secondary timber and CLST increases.

$$f_{m,CLT,k} = k_{m,CLT} f_{t,0,k}^{0.8} \qquad \text{Eq. 3.1a}$$

$$k_{m,CLT} = k_{sys,m} k_{CLT/GLT} k_{h,CLT} k_{CoV,t} \qquad \text{Eq. 3.1b}$$

$$k_{h,CLT} = \left(\frac{600}{h_c}\right)^{0.1} \qquad \text{Eq. 3.1c}$$

$$k_{CoV,t} = 1.67 exp\left(1.48 CoV_{ft}\right)(1.33 - 2.18 CoV_{fm}) \qquad \text{Eq. 3.1d}$$

where $k_{sys,m}$ =1.1 is a system effect factor due to mutually interaction of lamellae in the CLT element's main direction with not less than 4 pieces of sawn timber [79]; $k_{CLT/GLT}$=0.94 is an empirical factor considering the differences in homogenisation effects between CLT and glulam [80]; $k_{h,CLT}$ is the depth factor obtained from Jobstl et al. [80]; $k_{cov,t}$ is an adjustment factor based on the CoV of the base materials [77]; CoV_{ft} is the CoV of the tensile strength parallel to the grain, which was conservatively assumed to be the same as the CoV of the bending strength in Table 3.3; CoV_{fm} is the CoV of the bending strength of the CLT (Table 3.4).

Table 3.5 Comparison between results from testing and analytical modelling

Items		Test	γ-method	Error with tests	Shear analogy method	Error with tests
$(EI)_{eff}$ $(N\cdot mm^2)$		2.74×10^{11}	1.89×10^{11}	-31%	2.25×10^{11}	-18%
M $(kN\cdot m)$	f_b=14.0 MPa	12.13	7.11	-41%	7.49	-38%
	f_b=15.1 MPa		7.67	-37%	8.08	-33%
	f_b=19.3 MPa		10.41	-14%	10.97	-10%

4 Conclusions and outlook

This paper explored the possibility of using secondary timber as the feedstock to manufacture cross-laminated secondary timber (CLST). Non-destructive methods were used to assess the structural properties of both secondary timber and the CLST made from it. Destructive bending tests of secondary timber and full-scale CLST panels were conducted to validate the non-destructive methods and the feasibility of using CLST as structural members.

1) There was a good linear relationship (r^2 = 0.75) between the stiffness of secondary timber determined by non-destructive and destructive methods (dMoE and sMoE, respectively). The elastic modulus determined by non-destructive testing can therefore be used to predict the bending stiffness of secondary timber.
2) dMoE provided a less accurate prediction (r^2 = 0.23) for MoR due to the high variability of the latter. However, it is promising to predict MoR conservatively by combining dMoE and strength grade information in EN 338 [49].
3) The bending stiffness of CLST can be predicted more accurately by the average dMoE of the secondary timber pieces in the major direction (r^2 = 0.75) than the dMoE of the CLST as measured in transverse vibration tests (r^2 = 0.39).
4) Finger joints did not influence the bending performance of CLST made by relatively low-grade secondary timber. The structural properties of CLST could meet the bending strength and stiffness requirements from ANSI/APA PRG 320 [28], so CLST is a promising alternative structural product for the construction industry.
5) The analytical models in the Canadian CLT handbook provided a conservative means of predicting strength and stiffness of CLST. The accuracy of the estimate was further improved by considering the homogenisation effects through a bearing model.

Further research is also required to resolve the following questions:

1) More data are required to validate the suitability of referring strength grade in current standards during predicting secondary timber’s MoR, especially for stronger strength grades, such as C24, the mainstream feedstock for commercial CLT products.
2) The influence of finger joints and cracks on the accuracy of transverse vibration tests requires further investigation.
3) Tests including more timber species and grades are recommended to increase the knowledge base for the properties of secondary timber and its laminated products for practical use.
4) The suitability of the bearing model for secondary timber needs to be validated through more experimental tests.
5) Other properties, such as the rolling shear strength of CLST, need to be measured and compared with the product standards for CLT.

5 Acknowledgements

The authors would like to acknowledge the generous support of the Ramboll Foundation through the Flemming Bligaard Award, and University College London. The authors would also like to acknowledge Sir Robert McAlpine Ltd and Ramboll UK Ltd. for providing secondary timber used in the experimental work. The voluntary assistance from UCL students, Penghui Xu and Yue Pan, and technical support from Mark Burrows, Leslie Irwin, Ramanbhai Mangabhai, Warren Gaynor, Abishera Rajkumar and Shi Shi is also highly appreciated.

6 Nomenclature

CoV_{fm}	Coefficient of Variation (CoV) of bending strength of CLT
CoV_{ft}	CoV of tension strength parallel to grain
E_i	MoE of sawn timber in the major direction
$E_{j,90}$	MoE perpendicular to grain for the *j*-th layer in the minor direction
E_{mean}	Average MoE in the outermost layer of CLST panels
$(EI)_{eff}$	Effective bending stiffness of CLST panels
$(EI)_{eff,SA}$	Effective bending stiffness of CLST panels calculated by shear analogy method
$(EI)_{eff,gamma}$	Effective bending stiffness of CLST panels calculated by γ-method
F_1	10% of the estimated maximum load
F_2	40% of the estimated maximum load
F_m	Estimated maximum load
G	Shear modulus
G_{90}	Rolling shear stiffness
$G_{90,j}$	Rolling shear stiffness of the *j*-th layer in the minor direction
$I_{CL,net}$	Moment of inertia calculated from properties of the layers having its fibres parallel to span only
K_d	Factor according to different support conditions of vibration tests
W	Weight of the CLST panel
L	Length of the test piece
a	Distance between the loading point and its closest support

b	Cross-section width of the test piece
b_i	Width of the *i*-th layer in the major direction of CLST panels
b_j	Width of the *j*-th layer in the minor direction of CLST panels
b_c	Cross-section width of the CLST panel
$dMoE_{CL,T}$	dynamic Modulus of Elasticity (dMoE) of CLST panel through transverse vibration tests
$dMoE_{L,\alpha}$	Longitudinal dMoE at a moisture content α
$dMoE_{L,12\%}$	Longitudinal dMoE at a moisture content of 12%
f_L	Fundamental longitudinal vibration frequency
f_T	Fundamental transverse vibration frequency
$f_{m,CL,EU}$	Modulus of rupture of CLST panels according to Eurocode 5
$f_{m,CL,US}$	Modulus of rupture of CLST panels according to PRG 320
$f_{m,CLT,k}$	Characteristic bending strength of CLT
$f_{m,st}$	Modulus of rupture of secondary timber
h	Cross-section height of the test piece
h_c	Cross-section height of the CLST panel
h_i	Height of the *i*-th layer in the major direction of CLST panels
h_j	Height of the *j*-th layer in the minor direction of CLST panels
$k_{CLT/GLT}$	Empirical factor considering the differences in homogenisation effects between CLT and glulam
$k_{cov,t}$	Adjustment factor considering the CoV of materials
$k_{h,CLT}$	Depth factor
$k_{sys,m}$	System effect factor
l	Span of a specimen
l_1	Gauge length between measuring points of the CLST panel
l_2	Distance between the loading point and its closest support of the CLST panel
l_t	Total length of a specimen
r^2	Coefficient of determination

$sMoE_{CL}$ sMoE of CLST panels

$sMoE_g$ Global static modulus of elasticity

z_i Distance from the centroid of the *i*-th layer to the centroid of the cross-section

z_j Distance from the centroid of the *j*-th layer to the centroid of the cross-section

z_s Distance between the edge of CLST to the neutral axis

α Measured moisture content

$\alpha_{bt,j}$ Aspect ratio of the *j*-th layer in the minor direction

β_0 Intercept of the linear regression

β_1 Slope of the linear regression

γ_i Connection efficiency factor for the *i*-th layer

ρ Timber density

w_1 Middle span displacement at F_1

w_2 Middle span displacement at F_2

7 References

[1] Charlotte L, Eberhardt M, Birkved M, Birgisdottir H. Building design and construction strategies for a circular economy Building design and construction strategies for a circular economy. Architectural Engineering and Design Management 2022;18:93–113. https://doi.org/10.1080/17452007.2020.1781588.

[2] DEFRA. UK statistics on waste 2021. https://www.gov.uk/government/statistics/uk-waste-data/uk-statistics-on-waste (accessed January 18, 2023).

[3] Love E. WRA: four million tonnes of waste wood processed in 2021. Resource 2022. https://resource.co/article/wra-four-million-tonnes-waste-wood-processed-2021 (accessed January 18, 2023).

[4] Höglmeier K, Weber-Blaschke G, Richter K. Evaluation of wood cascading. Sustainability Assessment of Renewables-based Products: Methods and Case Studies 2015:335–46. https://doi.org/10.1002/9781118933916.ch22.

[5] Irle M, Privat F, Couret L, Belloncle C, Bonnin E, Cathala B, et al. Advanced recycling of post-consumer solid wood and MDF. Wood Material Science and Engineering 2019;0272. https://doi.org/10.1080/17480272.2018.1427144.

[6] Ramage MH, Burridge H, Busse-wicher M, Fereday G, Reynolds T, Shah DU, et al. The wood from the trees : The use of timber in construction. Renewable and Sustainable Energy Reviews 2017;68:333–59. https://doi.org/10.1016/j.rser.2016.09.107.

[7] Wood Recyclers'Association. UK Waste wood market goes from strength to strength exceeding 4 million tonnes of processed wood 2022. https://woodrecyclers.org/uk-waste-wood-market-goes-from-strength-to-strength-exceeding-4-million-tonnes-of-processed-wood/ (accessed January 18, 2023).

[8] Rose C. Systems for Reuse , Repurposing and Upcycling of Existing Building Components. University College London, 2019.

[9] Sandberg K, Sandin Y, Harte A, Shotton E, Hughes M, Ridley-Ellis D, et al. Summary report InFutUReWood – Innovative Design for the Future – Use and Reuse of Wood (Building) Components. 2022. https://doi.org/10.23699/p41e-ae46.

[10] Giordano L, Derikvand M, Fink G. Bending Properties and Vibration Characteristics of Dowel-Laminated Timber Panels Made with Short Salvaged Timber Elements. Buildings 2023;13:199. https://doi.org/10.3390/buildings13010199.

[11] Kohara J, Okamoto H. Studies of Japanese old timbers. Sci Rep Saikyo Univ 1955;7:9–20.

[12] Cavalli A, Cibecchini D, Togni M, Sousa HS. A review on the mechanical properties of aged wood and salvaged timber. Construction and Building Materials 2016;114:681–7. https://doi.org/10.1016/j.conbuildmat.2016.04.001.

[13] Falk R, Maul D, Cramer S, Evans J, Herian V. Engineering properties of douglas-fir lumber reclaimed from deconstructed buildings. vol. 650. 2008.

[14] Crews K, Mackenzie C. Development of grading rules for recycled timber used in structural applications. World Conference on Timber Engineering, 2008.

[15] British Standard Institution (BSI). BS EN 336: Structural Timber — Sizes, permitted deviations 2013.

[16] Risse M, Weber-blaschke G, Richter K. Science of the Total Environment Eco-ef fi ciency analysis of recycling recovered solid wood from construction into laminated timber products. Science of the Total Environment 2019;661:107–19. https://doi.org/10.1016/j.scitotenv.2019.01.117.

[17] Brandner R. Stochastic System Actions and Effects in Engineered Timber Products and

Structures. 2012.

[18] Concu G, De Nicolo B, Fragiacomo M, Trulli N, Valdes M. Grading of maritime pine from Sardinia (Italy) for use in cross-laminated timber. Proceedings of Institution of Civil Engineers: Construction Materials 2018;171:11–21. https://doi.org/10.1680/jcoma.16.00043.

[19] Rose CM, Bergsagel D, Dufresne T, Unubreme E, Lyu T, Duffour P, et al. Cross-Laminated Secondary Timber : Experimental Testing and Modelling the Effect of Defects and Reduced Feedstock Properties. Sustainability (Switzerland) 2018. https://doi.org/10.3390/su10114118.

[20] Fredriksson M, Bomark P, Broman O, Grönlund A. Using Small Diameter Logs for Cross-Laminated Timber Production. BioResources 2015;10:1477–86.

[21] Lawrence C. Utilization of Low-value Lumber from Small-diameter Timber Harvested in Pacific Northwest Forest Restoration Programs in Hybrid Cross Laminated Timber (CLT) Core Layers: Technical Feasibility. Oregon State University, 2017.

[22] Jahedi S. Defining Project-Specific Custom CLT Grade Utilizing Low-Value Ponderosa Pine Lumber from Logs Harvested in SW Oregon and Northern California Forest Restoration Programs. Oregon State University, 2022.

[23] Bhandari S, Jahedi S, Riggio M, Muszynski L. CLT modular low-rise buildings: A DfMA approach for deployable structures using low-grade timber. World Conference on Timber Engineering, Chile: 2021.

[24] Ma Y, Si R, Musah M, Dai Q, Xie X, Wang X, et al. Mechanical Property Evaluation of Hybrid Mixed-Species CLT Panels with Sugar Maple and White Spruce. Journal of Materials in Civil Engineering 2021;33. https://doi.org/10.1061/(asce)mt.1943-5533.0003760.

[25] Urban Machine n.d. https://urbanmachine.build/ (accessed January 18, 2023).

[26] Stenstad A, Bertelsen SL, Modaresi R. Comparison of strength tests for evaluating the secondary timber utilisation in Cross Laminated Timber (CLT). WCTE 2021 - World Conference on Timber Engineering 2021:1–6.

[27] Arbelaez R. Exploratory Study of Salvaged Lumber as Feedstock for Cross-Laminated Timber (CLT). Oregon State University, 2019.

[28] APA-The Engineered Wood Association. ANSI/APA PRG 320-2018 Standard for

performance-rated cross-laminated timber. Tacoma, WA: APA-The Engineered Wood Association 2018.

[29] Ma Y, Wang X, Begel M, Dai Q, Dickinson Y, Xie X, et al. Flexural and shear performance of CLT panels made from salvaged beetle-killed white spruce. Construction and Building Materials 2021;302. https://doi.org/10.1016/j.conbuildmat.2021.124381.

[30] Llana DF, González-Alegre V, Portela M, Íñiguez-González G. Cross Laminated Timber (CLT) manufactured with European oak recovered from demolition: Structural properties and non-destructive evaluation. Construction and Building Materials 2022;339:127635. https://doi.org/10.1016/j.conbuildmat.2022.127635.

[31] Azeez AA. Evaluating the Suitability of Salvaged Lumber as Feedstock in Cross-Laminated Timber. Michigan State University, 2022.

[32] Chúláin CU, Llana DF, Hogan P, McGetrick P, Harte AM. Bending characteristics of CLT from recovered spruce. World Conference on Timber Engineering 2023, 2023, p. 888–94.

[33] Li H, Wang L, Wang BJ, Wei P, Yu W, Fan Z, et al. Preliminary evaluation of a density-based lumber grading method for hem-fir CLT manufacturing. European Journal of Wood and Wood Products 2021. https://doi.org/10.1007/s00107-020-01653-3.

[34] Unterwieser H, Schickhofer G. Characteristic values and test configurations of CLT with focus on selected properties. COST Action FP1004: Focus Solid Timber Solutions-European Conference on Cross Laminated Timber (CLT) 2013:53–73.

[35] Osuna-sequera C, Llana DF, Íñiguez-gonzález G, Arriaga F. The influence of cross-section variation on bending stiffness assessment in existing timber structures. Engineering Structures 2020;204:110082. https://doi.org/10.1016/j.engstruct.2019.110082.

[36] Cavalli A, Bevilacqua L, Capecchi G, Cibecchini D, Fioravanti M, Goli G, et al. MOE and MOR assessment of in service and dismantled old structural timber. Engineering Structures 2016;125:294–9. https://doi.org/10.1016/j.engstruct.2016.06.054.

[37] Smith MJ. An investigation into the strength properties of reclaimed timber joists. Northumbria University, 2012.

[38] Jia R, Wang Y, Wang R, Chen X. Physical and Mechanical Properties of Poplar Clones and Rapid Prediction of the Properties by Near Infrared Spectroscopy. Forests 2021:1–

14. https://doi.org/10.3390/f12020206.

[39] Skowroński W, Stawiski B. Ultrasonic evaluation regarding the effects of biological corrosion of historical roof trusses. MATEC Web of Conferences, vol. 284, EDP Sciences; 2019, p. 7006.

[40] Kranitz K, Deulein M, Niemz P. Determination of dynamic elastic moduli and shear moduli of aged wood by means of ultrasonic devices. Materials and Structures 2014;47:925–36. https://doi.org/10.1617/s11527-013-0103-8.

[41] Xin Z, Fu R, Zong Y, Ke D, Zhang H. Effects of natural ageing on macroscopic physical and mechanical properties , chemical components and microscopic cell wall structure of ancient timber members. Construction and Building Materials 2022;359:129476. https://doi.org/10.1016/j.conbuildmat.2022.129476.

[42] Xin Z, Ke D, Zhang H, Yu Y, Liu F. Non-destructive evaluating the density and mechanical properties of ancient timber members based on machine learning approach. Construction and Building Materials 2022;341:127855. https://doi.org/10.1016/j.conbuildmat.2022.127855.

[43] Arriaga F, Osuna-sequera C, Bobadilla I, Esteban M. Prediction of the mechanical properties of timber members in existing structures using the dynamic modulus of elasticity and visual grading parameters. Construction and Building Materials 2022;322. https://doi.org/10.1016/j.conbuildmat.2022.126512.

[44] Carrillo M, Carreón H. Study of the Degradation Effects on Aged Wood Beams from the Cathedral of Morelia, Mexico by Acoustic Birefringence Measurements. Russian Journal of Nondestructive Testing 2020;56:1042–9. https://doi.org/10.1134/S1061830921010034.

[45] Concu G, De Nicolo B, Riu R, Trulli N, Valdes M, Fragiacomo M. Sonic testing on cross laminated timber panels. Proceeding of the 6th International Conference on Structural Engineering, Mechanics and Computation-Insights and Innovations in Structural Engineering, Mechanics and Computation, Cape Town, South Africa, 2016.

[46] Gsell D, Feltrin G, Schubert S, Steiger R, Motavalli M. Cross-Laminated Timber Plates : Evaluation and Verification of Homogenized Elastic Properties. Journal of Structural Engineering 2007;133:132–8. https://doi.org/10.1061/(ASCE)0733-9445(2007)133.

[47] Steiger R, Gülzow A, Gsell D. Non destructive evaluation of elastic material properties of crosslaminated timber (CLT). Conference COST E, vol. 53, Citeseer; 2008, p. 29–30.

[48] Opazo-vega A, Benedetti F, Nuñez-decap M, Maureira-carsalade N, Oyarzo-vera C. Non-Destructive Assessment of the Elastic Properties of Low-Grade CLT Panels. Forests 2021;12:1734. https://doi.org/https://doi.org/10.3390/f12121734.

[49] British Standard Institution (BSI). BS EN 338:2016: Structural timber. Strength classes 2016.

[50] British Standard Institution (BSI). BS EN 519:1995-Structural timber-Grading-Requirements for machine strength graded timber and grading machines.pdf 1995.

[51] Mississippi State University. Smart Thumper n.d. https://www.smartthumper.fwrc.msstate.edu/.

[52] Turkot CG. Preliminary characterization of physical and mechanical properties of species used in staircase manufactures. Mississippi State University, 2019.

[53] Kumar C, Redman A, Leggate W, Mcgavin RL. Assessment of the Application of a SMART THUMPER ™ as a Low-cost and Portable Device Used for Stiffness Estimation of Timber Products. BioResources 2021;16:5838–61.

[54] ASTM standard. ASTM E1876-21 Standard Test Method for Dynamic Young's Modulus, Shear Modulus, and Poisson's Ratio by Impulse Excitation of Vibration 2021.

[55] British Standard Institution (BSI). BS EN 384:2016+A1:2018+A2:2022 Structural timber - Determination of characteristic values of mechanical properties and density 2018.

[56] Evans JW, Kretschmann DE, Herian VL, Green DW. Procedures for Developing Allowable Properties for a Single Species Under ASTM D1990 and Computer Programs Useful for the Calculations. 2001.

[57] Franca FJN, Seale RD, Shmulsky R, Franca TSFA. Assessing Southern Pine 2x4 and 2x6 Lumber Quality : Longitudinal and Transverse Vibration. Wood and Fiber Science 2019;51:1–14. https://doi.org/10.22382/wfs-2019-002.

[58] British Standard Institution (BSI). BS EN 408: 2010 Timber structures — Structural timber and glued laminated timber — Determination of some physical and mechanical properties 2012.

[59] Nocetti M, Bacher M, Brunetti M, Crivellaro A. Relationship between local and global modulus of elasticity in bending and its consequence on structural timber grading. European Journal of Wood and Wood Products 2013:297–308.

https://doi.org/10.1007/s00107-013-0682-7.

[60] ASTM standard. ASTM D6874-21 Standard Test Methods for Nondestructive Evaluation of the Stiffness of Wood and Wood-Based Materials Using Transverse Vibration or Stress Wave Propagation 2021. https://doi.org/10.1520/D6874-21.2.

[61] Zhang L, Tiemann A, Zhang T, Gauthier T, Hsu K, Mahamid M, et al. Nondestructive assessment of cross - laminated timber using non - contact transverse vibration and ultrasonic testing. European Journal of Wood and Wood Products 2021;79:335–47. https://doi.org/10.1007/s00107-020-01644-4.

[62] British Standard Institution (BSI). BS EN 16351:2021 Timber structures — Cross laminated timber — Requirements 2021.

[63] Corpataux L, Okuda S, Kua HW. Panel and plate properties of Cross-laminated timber (CLT) with tropical fast-growing timber species in compliance with Eurocode 5. Construction and Building Materials 2020;261:119672. https://doi.org/10.1016/j.conbuildmat.2020.119672.

[64] British Standard Institution (BSI). Eurocode 5: design of timber structures—Part 1-1: General—Common rules and rules for buildings 2004.

[65] American Society for Testing and Materials. ASTM D198-22a Standard Test Methods of Static Tests of Lumber in Structural Sizes 2022. https://doi.org/10.1520/D0198-22a.Copyright.

[66] Pang SJ, Shim KB, Kim KH. Effects of knot area ratio on the bending properties of cross-laminated timber made from Korean pine. Wood Science and Technology 2021;55:489–503. https://doi.org/10.1007/s00226-020-01255-5.

[67] Karacabeyli E, Gagnon S. Canadian CLT handbook. 2019th ed. National Library of Canada; 2019.

[68] Ehrhart T, Brandner R, Schickhofer G, Frangi A. Rolling shear properties of some European timber species with focus on cross laminated timber (CLT): Test configuration and parameter study; Paper 48-6-1. International Network on Timber Engineering Research (INTER), 2015.

[69] Yang BZ, Seale RD, Shmulsky R, Dahlen J, Wang X. Comparison of nondestructive testing methods for evaluating No.2 southern pine lumber: part A, modulus of elasticity. Wood and Fiber Science 2015;47:375–84.

[70] Liliefna LD. Structural property relationships for Canadian dimension lumber. University of British Columbia, 1994.

[71] American Society for Testing and Materials. ASTM D1990-19：Standard Practice for Establishing Allowable Properties for Visually-Graded Dimension Lumber from In-Grade Tests of Full-Size Specimens 2019. https://doi.org/10.1520/D1990-19.ogy.

[72] British Standard Institution (BSI). EN 14081-1 +A1 2019 Timber Structures–Strength Graded Structural Timber with Rectangular Cross Section–Part 1: General Requirements 2016.

[73] Yang BZ, Seale RD, Shmulsky R, Dahlen J, Wang X. Comparison of nondestructive testing methods for evaluating No 2 southern pine lumber: part B, modulus of rupture. Wood and Fiber Science 2017;49:134–45.

[74] British Standard Institution (BSI). EN 14358: 2016, Timber structures–Calculation and verification of characteristic values 2016.

[75] Huang Z. Residual strength and stiffness of waste timber: potential for exploitation to produce cross-lamianted timber. University College London, 2019.

[76] He M, Sun X, Li Z. Bending and compressive properties of cross-laminated timber (CLT) panels made from Canadian hemlock. Construction and Building Materials 2018;185:175–83. https://doi.org/10.1016/j.conbuildmat.2018.07.072.

[77] Brandner R, Schickhofer G. Glued laminated timber in bending: new aspects concerning modelling. Wood Science and Technology 2008;42:401–25. https://doi.org/10.1007/s00226-008-0189-2.

[78] Brandner R, Flatscher G, Ringhofer A, Schickhofer G, Thiel A. Cross laminated timber (CLT): overview and development. European Journal of Wood and Wood Products 2016;74:331–51. https://doi.org/10.1007/s00107-015-0999-5.

[79] Brandner R, Schickhofer G. System effects of structural elements-determined for bending and tension. proceedings of the 9th World Conference on Timber Engineering (WCTE 2006), Portland, 2006.

[80] Jöbstl R-A, Bogensperger T, Moosbrugger T, Schickhofer G. A Contribution to the Design and System Effect of Cross Laminated Timber. CIB W18, 39th Meeting, .; 2006.